

Supporting Information

Thulium- and Erbium-Doped Nanoparticles with Poly(acrylic acid) Coating for Upconversion Cross- Correlation Spectroscopy-based Sandwich Immunoassays in Plasma

Satu Lahtinen^{‡,†}, Mikkel Baldtzer Liisberg^{‡,‡}, Kirsti Raiko,[†] Stefan Krause,^{*} Tero Soukka,[†]
and Tom Vosch[‡]*

[†] Department of Biotechnology, University of Turku, Kiinamyllynkatu 10, 20520 Turku,
Finland

[‡] Nano-Science Center, Department of Chemistry, University of Copenhagen,
Universitetsparken 5, 2100 Copenhagen, Denmark

^{*} Department of Chemistry, Ludwig-Maximilians University of Munich, Butenandtstr. 5-13,
81377 Munich, Germany

[‡] These authors contributed equally to this work

Corresponding Author

*selaht@utu.fi

Table of Contents

TEM images of PAA-coated UCNPs.....	S3
Filtration experiment of antibody conjugated UCNPs incubated in plasma.....	S4
TEM images of the synthesized UCNPs.....	S4
Optical characterization of 3% and 20% Er-doped UCNPs.....	S5
Cross-talk of Er and Tm channels.....	S6
UCCS data in buffer with 3.2 $\mu\text{g/mL}$ UCNP concentration.....	S7
UCCS data in plasma with 3.2 $\mu\text{g/mL}$ UCNP concentration.....	S7
UCCS immunoassay data analysis.....	S8
Immunoassay standard curve fitting parameters.....	S14
Autocorrelation amplitudes in TSH immunoassay at 72 $\mu\text{g/mL}$ UCNP concentration.....	S14
Autocorrelation amplitudes in TSH immunoassay at 3.2 $\mu\text{g/mL}$ UCNP concentration.....	S15
References.....	S15

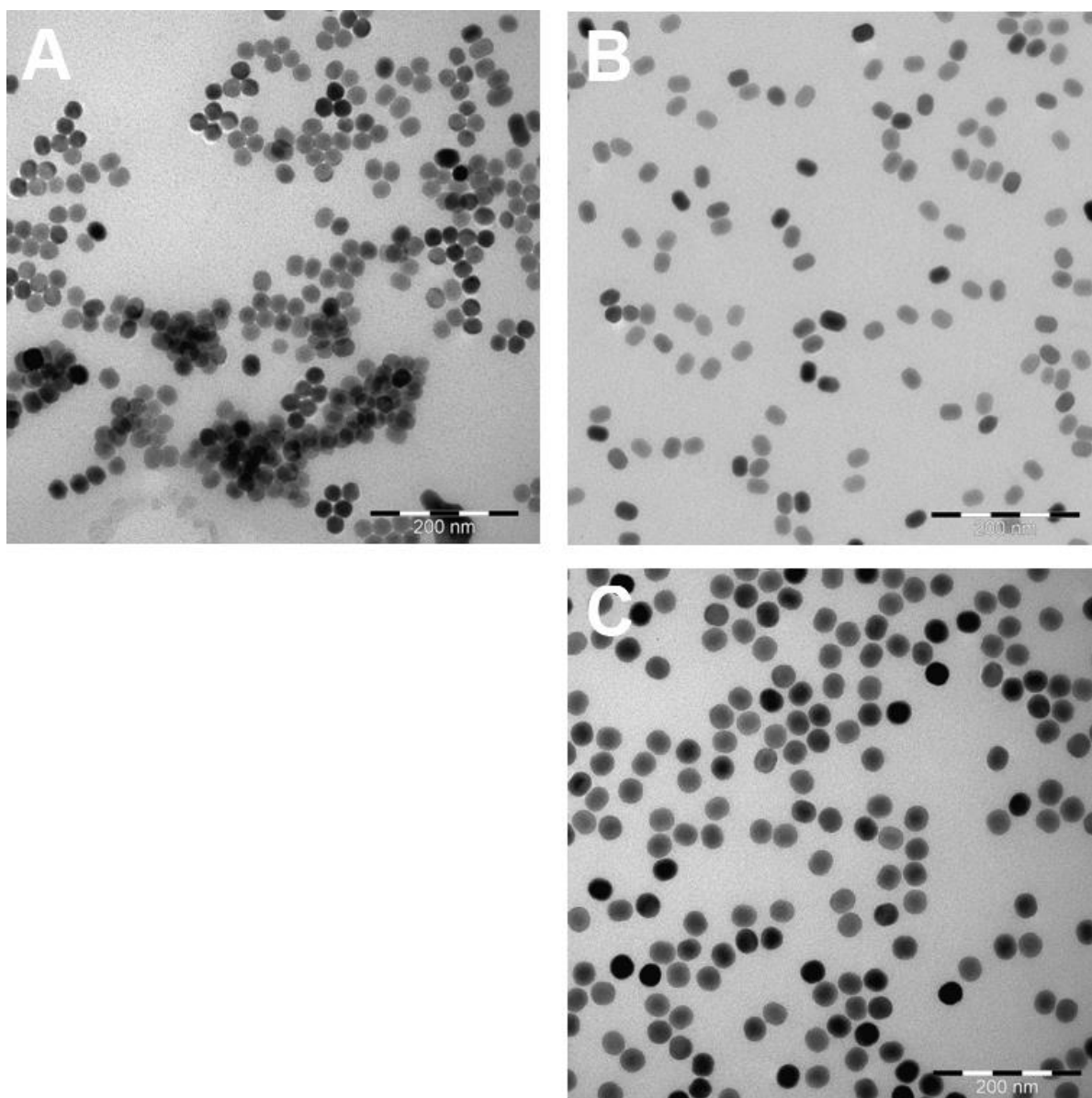


Figure S1. TEM-images of PAA-coated and antibody conjugated $\text{NaYF}_4:\text{Yb}^{3+},\text{Er}^{3+}$ (3% Er) UCNP, which were surface modified by A) HCl treatment and PAA coating in water or B) NOBF_4 ligand exchange and PAA coating in DMF at elevated temperature, and C) PAA-coated and antibody conjugated $\text{NaYF}_4:\text{Yb}^{3+},\text{Tm}^{3+}$ (8% Tm) UCNP, which were surface modified by using NOBF_4 ligand exchange and PAA coating in DMF at elevated temperature. All the TEM-samples of antibody conjugated UCNP have been made from water based UCNP dispersions. The scale bar is 200 nm.

Table S1. UCNP concentrations before and after filtrating the particles incubated in 20% plasma through different pore size filters. Standard deviations are based on six replicates.

		Surface modification	
		HCl + PAA in water	NOBF ₄ + PAA in DMF
UCNP concentration (µg/mL)	non-filtered	540 ± 91	200 ± 1
	220 nm filter	blocked	190 ± 1
	100 nm filter	N/A*	180 ± 9
Total loss in concentration (%)		100	10

* As the 220 nm filter was blocked and there was no flow through, the solution could not be filtered through 100 nm pore size filter

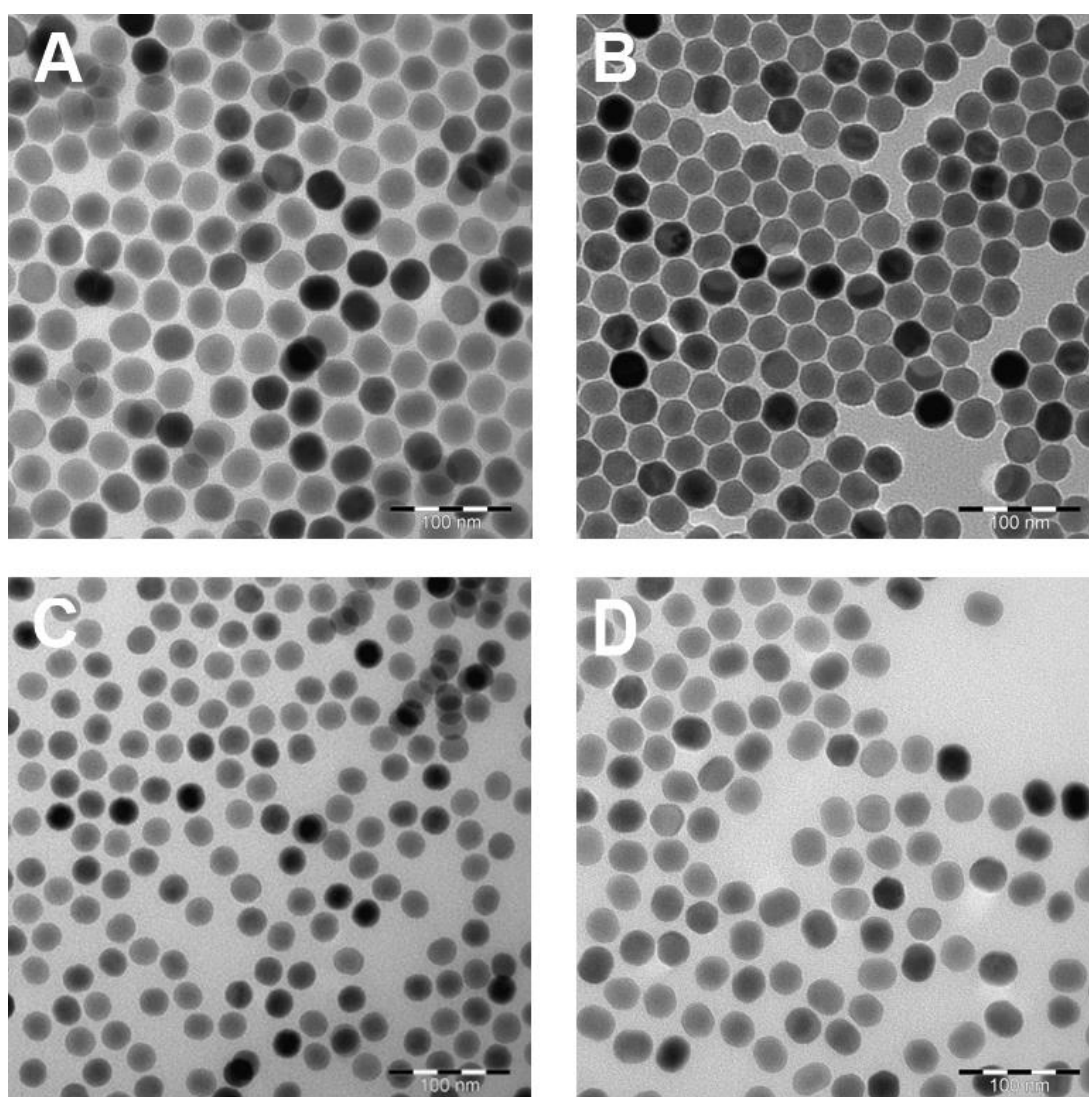


Figure S2. TEM-images of NaYF₄:Yb³⁺, Tm³⁺ UCNPs with A) 8% Tm, or B) 0.5% Tm (image published previously in SI of Lahtinen et al.¹), and NaYF₄:Yb³⁺, Er³⁺ UCNPs with C) 20% Er or D) 3% Er image with JEM-1400 Plus TEM (80 kV electron beam, JEOL, Massachusetts, USA). Scale bar is 100 nm.

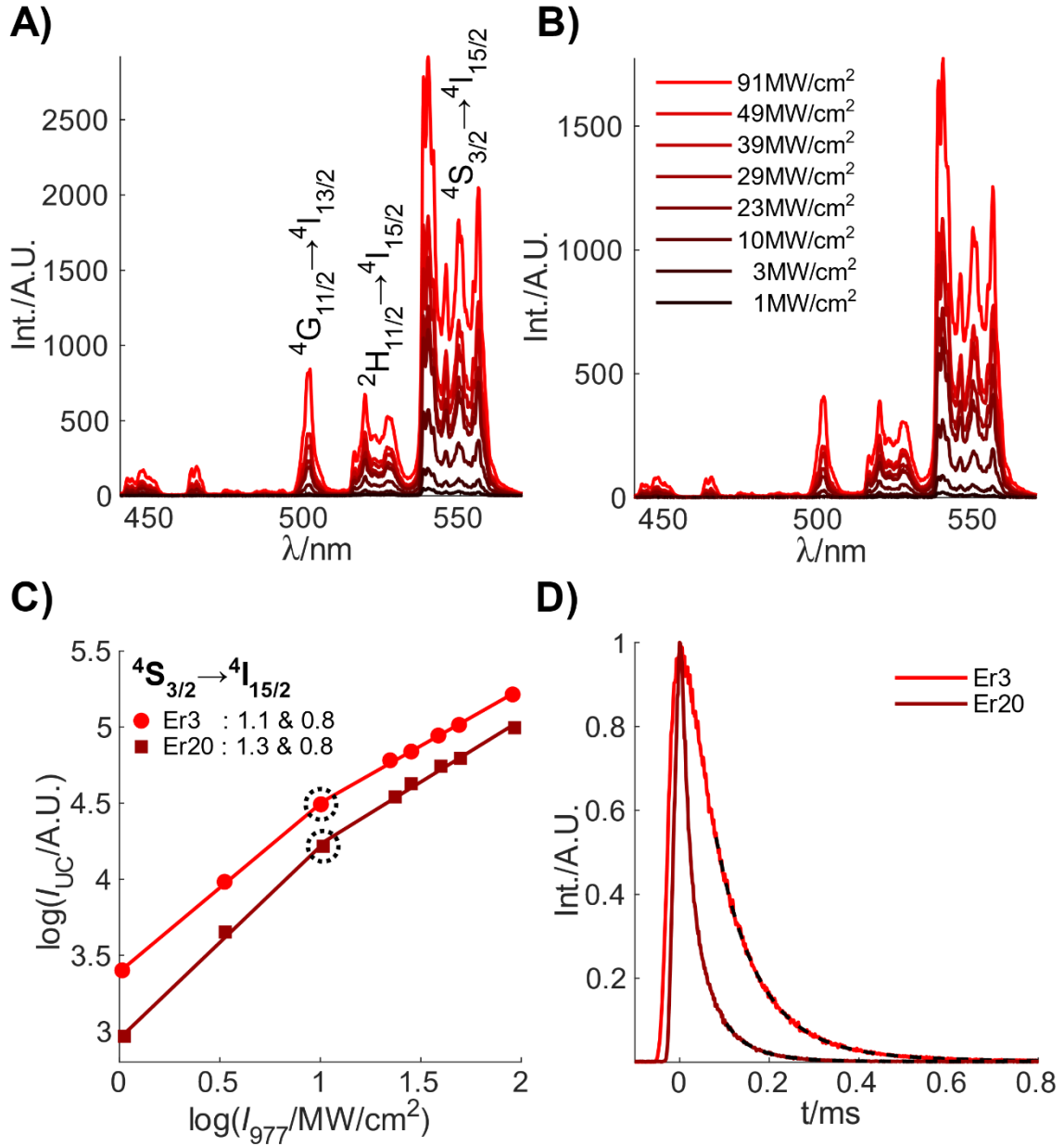


Figure S3. Optical characterization for low and high doped Er particles. Spectral power dependence of A) Er(3%) and B) Er(20%). The laser intensities used for Er(3%) are similar to those used for Er(20%) within 3%. C) Power dependence of the $4S_{3/2} \rightarrow 4I_{15/2}$ transition for both the low and high doped Er particles. Data points marked with a dashed circle indicate transitions between different power dependent regimes for Er(3%) and Er(20%). Two different slopes are fitted for Er(3%) and Er(20%) in these high and low power regimes and noted in the figure. D) Decay time measurements of the $4S_{3/2} \rightarrow 4I_{15/2}$ transition for Er(3%) and Er(20%).

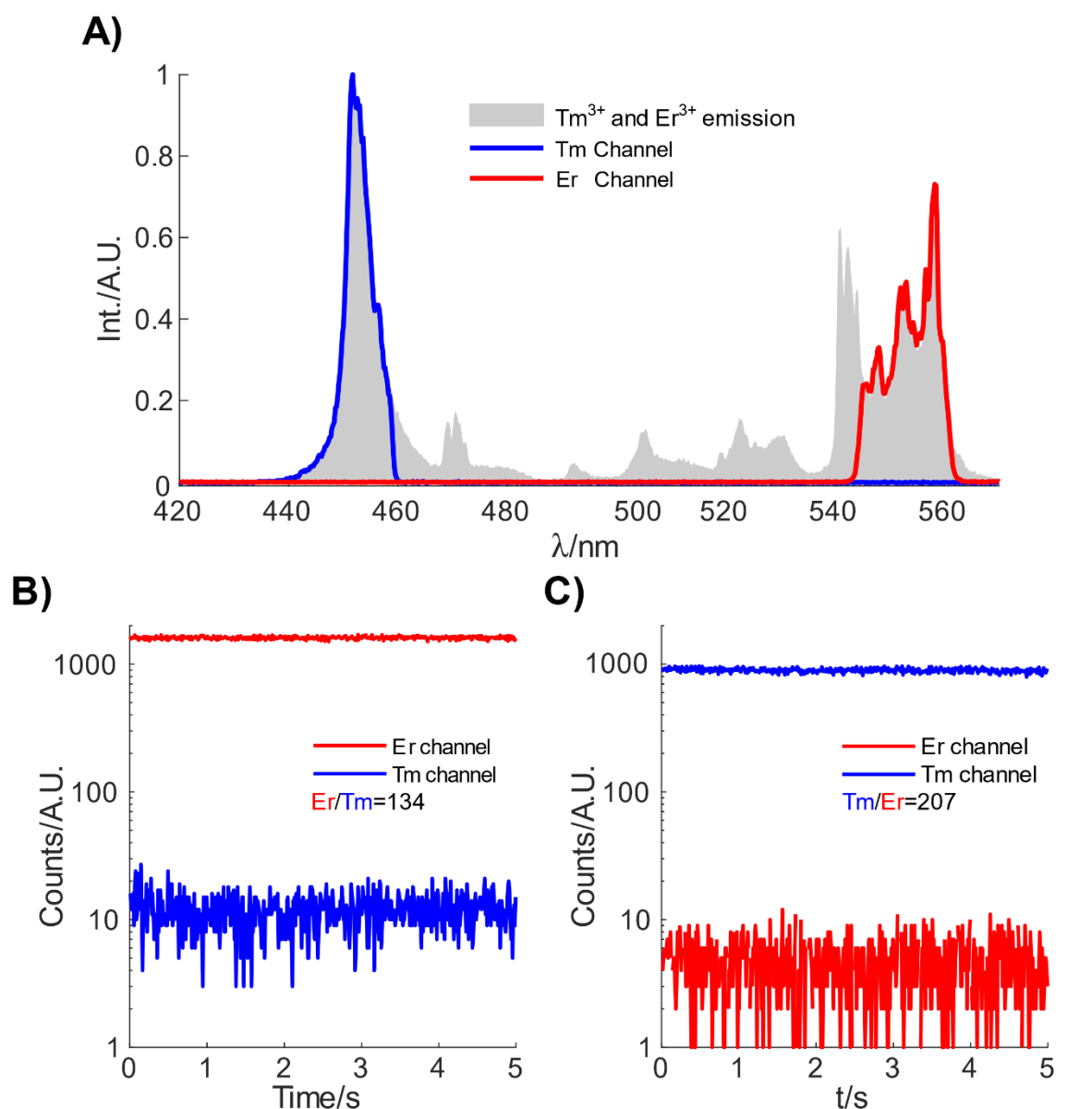


Figure S4. Cross-talk measurements. A) Region shown in grey corresponds to the spectrum obtained for a solution containing Tm(8%) and Er(3%) particles without any optical filters. The region shown in blue corresponds to the spectral region being probed for the Tm channel, and the red region corresponds to the Er channel. The “Tm and Er channel” spectra are obtained from the same solution but with the proper filter settings. A subsequent normalization is performed for both the Tm and Er channel such that the intensity of the individual channels overlay that of the combined emission spectrum (grey area). B) Intensity time trace measuring both the Er and Tm channel on a dried droplet from the Er(3%) stock solution with dark counts removed from the traces. A ratio between the average intensity of the Er channel compared to the Tm channel yields a ratio of 134. C) Similar to B), but now being performed on a dried droplet of Tm(8%) stock solution. This yields a ratio (Tm/Er) of 207.

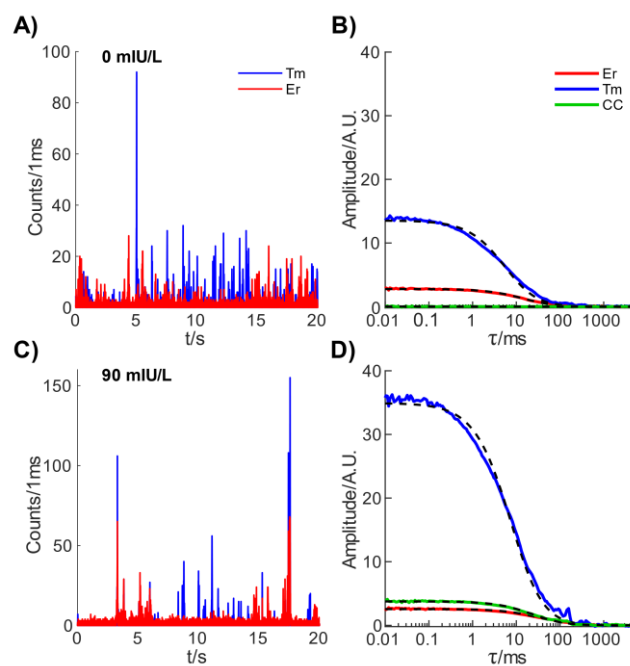


Figure S5. Section of a 300 s intensity time trace of Tm(8%) and Er(3%) particles (UCNP concentrations of 3.2 $\mu\text{g/mL}$) in the TSH immunoassay A) in buffer solution without TSH and C) in buffer solution spiked with 90 mIU/L TSH. Corresponding auto-correlation functions of the Er(3%) and Tm(8%) as well as the cross-correlation functions can be seen in B) and D).

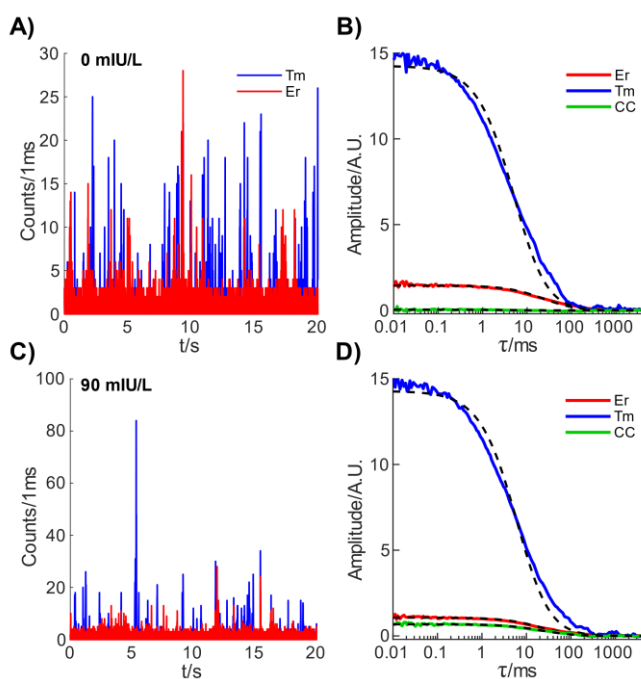


Figure S6. Section of a 300 s intensity time trace of Tm(8%) and Er(3%) particles (UCNP concentrations of 3.2 $\mu\text{g/mL}$) in the THS immunoassay A) in a plasma solution without TSH and C) in a plasma solution spiked with 90 mIU/L TSH. Corresponding auto-correlation functions of the Er(3%) and Tm(8%) as well as the cross-correlation functions can be seen in B) and D).

Upconversion cross-correlation immunoassay data analysis

Auto- and cross-correlation of the acquired data was performed with the Burst Analyzer 2 software (Becker & Hickl). Some treatment of the intensity time traces prior to correlating the data was performed in order to negate the effect of bright cross-linked species, which would otherwise affect the correlation curve. To remedy this issue, two different approaches were investigated for the high and low UNCP concentration series; either removing the obstructing cross-linked emission manually or by setting a threshold value. Deciding upon which features to remove manually was based on the relative brightness of the emissive species and the resulting auto- or cross-correlation curve, *i.e.* the appearance of shoulders at large time delays, τ , indicate the existence of slowly diffusing cross-linked species. The fitting of auto- and cross-correlation curves for the data treated with a manual removal was done in Burst Analyzer 2. The threshold approach necessitates deciding upon a certain value for a given binning time. For the first buffer series, where the high particle concentration results in high count rates, threshold values for either the Er or Tm channel of 400, 300, and 200 counts were used for a binning time of 1 ms. For the second buffer series, threshold values of 200, 150, and 100 counts for binning times of 1 ms are instead used due to the lower count rates. For both series and channels a flank level of 50 counts was used. The flank level defines the count level an intense burst has to reach before it is no longer excluded from the time trace. Fitting of auto- and cross-correlation curves treated with a threshold was done in MATLAB.

The effect of removing the luminescent bursts due to cross-linked species can be seen for the high UNCP concentration (72 $\mu\text{g/mL}$) in buffer in Figure S7. Large intensity bursts can be seen in the time trace in Figure S7A, and upon examining the resulting auto- and cross-correlation curves when no data treatment is applied, it is obvious from the shoulders at around 500 ms that these bursts are due to large cross-linked species. Most of the features from the cross-linked species in the correlation curves are excluded upon removal of the bright bursts by a manual or threshold approach. Auto- and cross-correlation amplitudes are extracted from fits to a simple 3D diffusion model according to equation (1)² at the investigated range of TSH concentrations (0 - 90 mIU/L) under the different data treatment conditions; Figure S8 and Figure S9 show the cross- and auto-correlation amplitudes as a function of the TSH concentration.

$$G(\tau) = A_{CC} \cdot \left(1 + \frac{\tau}{\Delta\tau}\right)^{-3/2} \quad (1)$$

While no data treatment yields significantly different results, there are only minor differences between the results obtained when treating the data manually or with a threshold. This is also reflected in the obtained LoDs given in Table S2. Based on these results, a threshold value of 400 counts was used for the preparation of the standard curve and exemplary auto- and cross-correlation curves for the high UNCP concentration in buffer and plasma shown in the main article, though deciding upon a particular threshold value appears to have little bias on the results.

Table S2. Limit of detections of TSH in UCCS immunoassay for high UCNP concentrations (72 $\mu\text{g/mL}$) in buffer obtained by treating the data at different conditions.

Approach	None	Manual removal	400 counts	300 counts	200 counts
LoD (mIU/L)	44.1	3.3	1.7	1.6	2.0

A similar analysis was conducted for the low UCNP concentration (3.2 $\mu\text{g/mL}$) in buffer. Figure S10 shows the effect of removing emission from cross-linked species upon the resulting correlation functions, with similar results as for the high UCNP concentration buffer series. Cross- and auto-correlation amplitudes as a function of TSH concentration under different data treatment conditions are shown in Figure S11 and Figure S12, respectively. The resulting LoDs can be seen in Table S3. While the no data treatment approach yields the best LoD, it is, however, still preferable to exclude any potential obstructing cross-linked species by a threshold, that might otherwise render a measurement unusable (see *e.g.*, the large auto-correlation amplitude deviations of erbium). In the main article, a threshold of 200 counts was accordingly used for the analysis of the low UCNP concentration data in both buffer and plasma.

Table S3. Limit of detections of TSH in UCCS immunoassay for low UCNP concentrations (3.2 $\mu\text{g/mL}$) in buffer obtained by treating the data at different conditions.

Approach	None	Manual removal	200 counts	150 counts	100 counts
LoD (mIU/L)	0.21	0.24	0.32	0.36	0.45

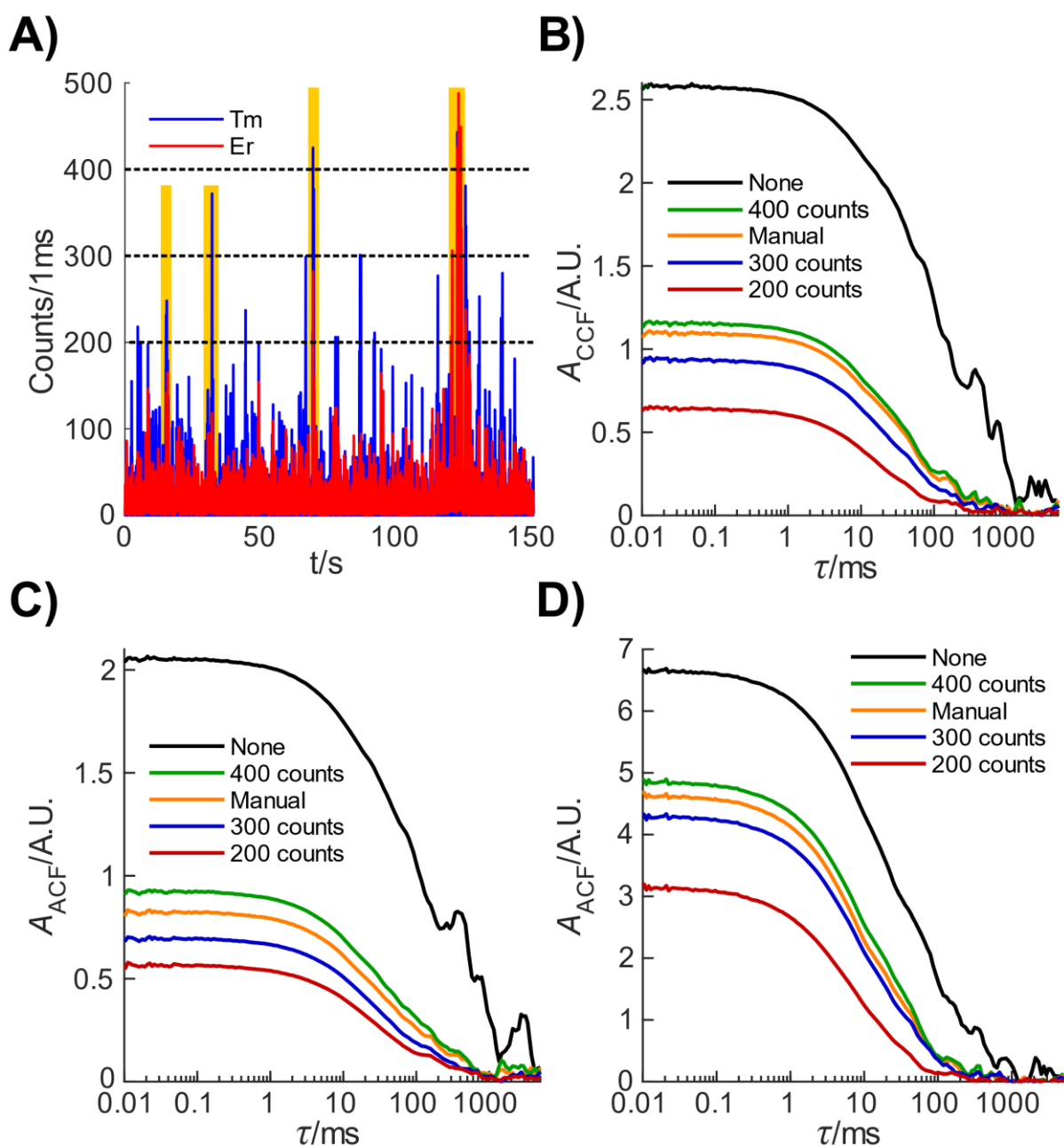


Figure S7. The effect of removing emission from cross-linked species upon the resulting correlation functions in the UCCS immunoassay at a high UCNP concentration (72 $\mu\text{g/mL}$). A) An intensity time trace from the 90 mIU/L TSH concentration showing the removal of data by defining a threshold (dashed lines) or by manually picking (yellow areas) out timespans with obstructing emission. B) Cross-correlation functions calculated from the intensity time traces in A) without any defined threshold, with a threshold of 400, 300, or 200 counts, or finally by manually removing emission stemming from cross-linked particles. C) Auto-correlation functions for the erbium channel from the time trace in A). D) Auto-correlation functions for the thulium channel from the time trace in A).

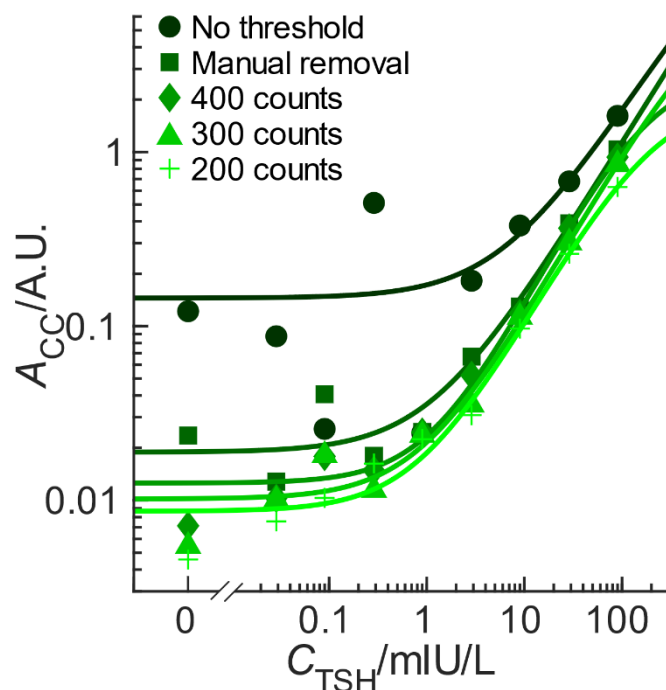


Figure S8. Standard curves for the TSH immunoassay at a high UCNP concentration (72 $\mu\text{g/mL}$) resulting from different data treatment approaches. The A_{CC} values represent the average of six replicate measurements.

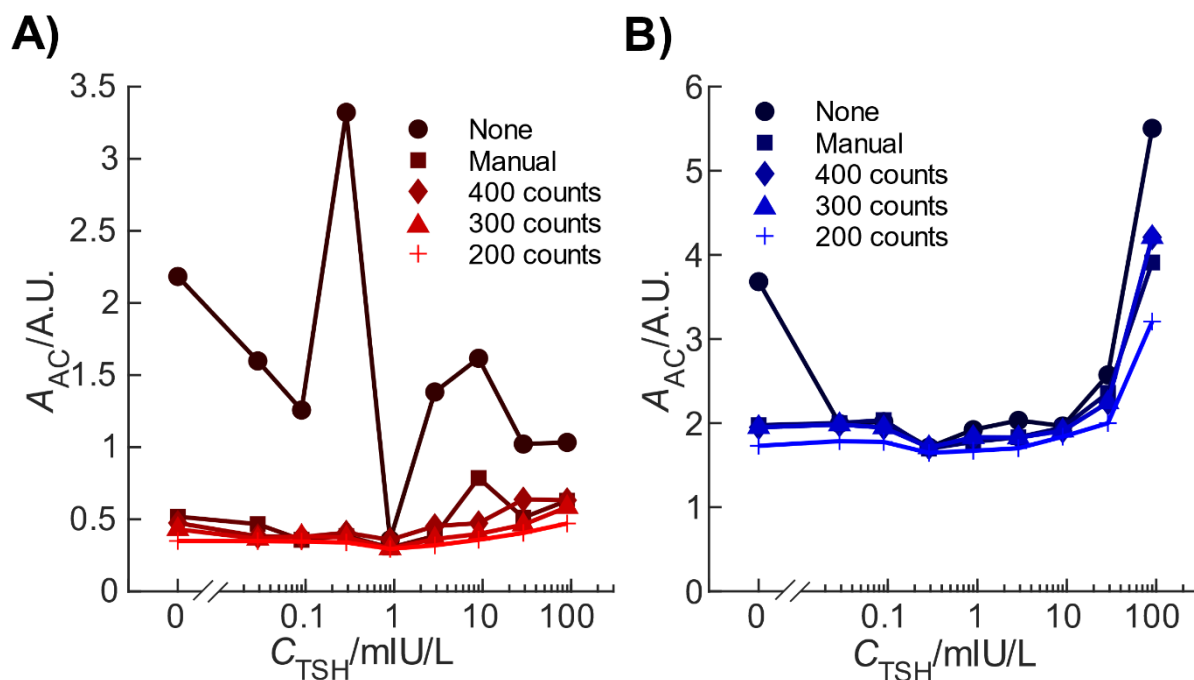


Figure S9. Amplitude of the auto-correlation function of A) erbium and B) thulium at different analyte concentrations and at a high UCNP concentration (72 $\mu\text{g/mL}$) in the TSH immunoassay. The A_{AC} values represent the average of six replicate measurements. There are large deviations when no threshold is used, while only minor differences are observed when a certain threshold is used.

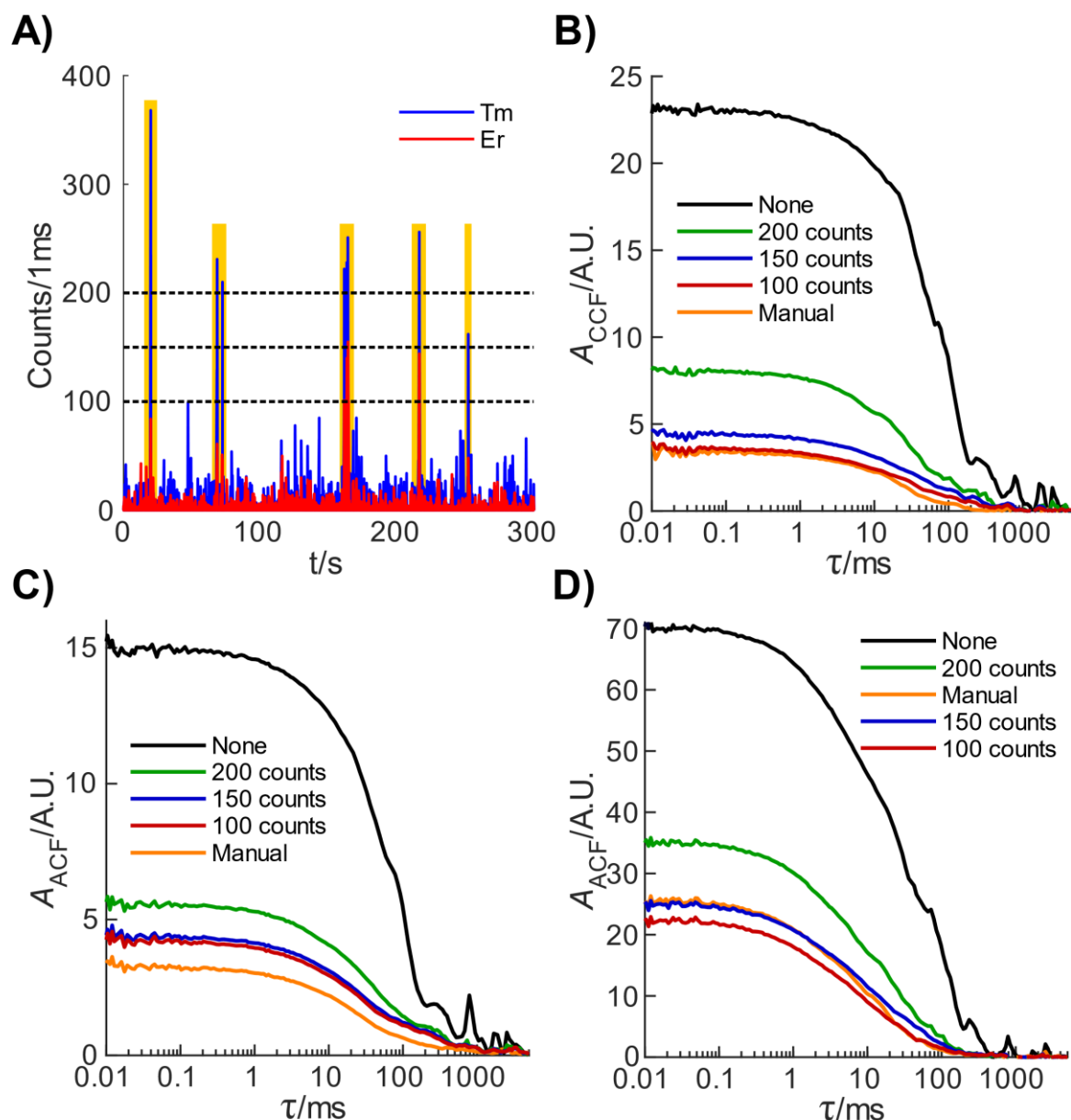


Figure S10. The effect of removing emission from cross-linked species upon the resulting correlation functions in the UCCS immunoassay at a low UCNP concentration (3.2 $\mu\text{g/mL}$). A) An intensity time trace from the 90 mIU/L TSH concentration showing the removal of data by defining a threshold (dashed lines) or by manually picking (yellow areas) out timespans with obstructing emission. B) Cross-correlation functions calculated from the intensity time traces in A) without any defined threshold, with a threshold of 200, 150, or 100 counts, or finally by manually removing emission stemming from cross-linked particles. C) Auto-correlation functions for the erbium channel from the time trace in A). D) Auto-correlation functions for the thulium channel from the time trace in A).

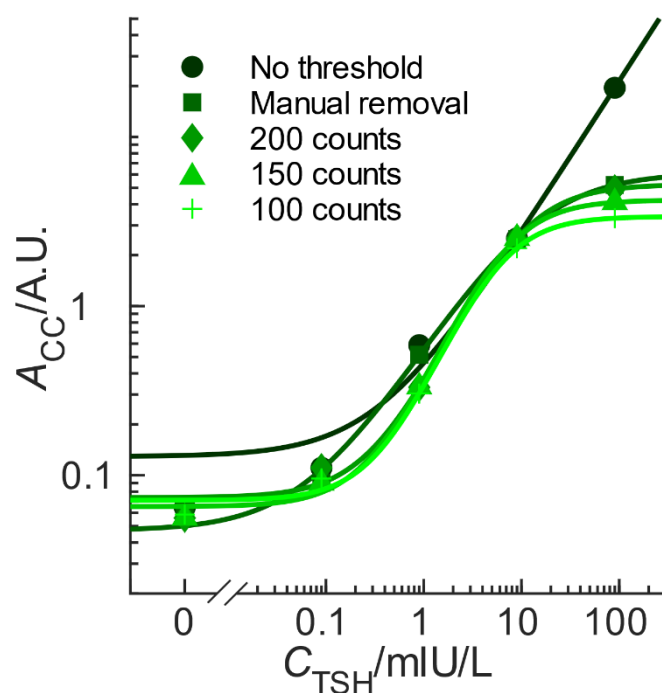


Figure S11. Standard curves for the TSH immunoassay at a low UCNP concentration (3.2 µg/mL) resulting from different data treatment approaches. The A_{CC} values represent the average of six replicate measurements.

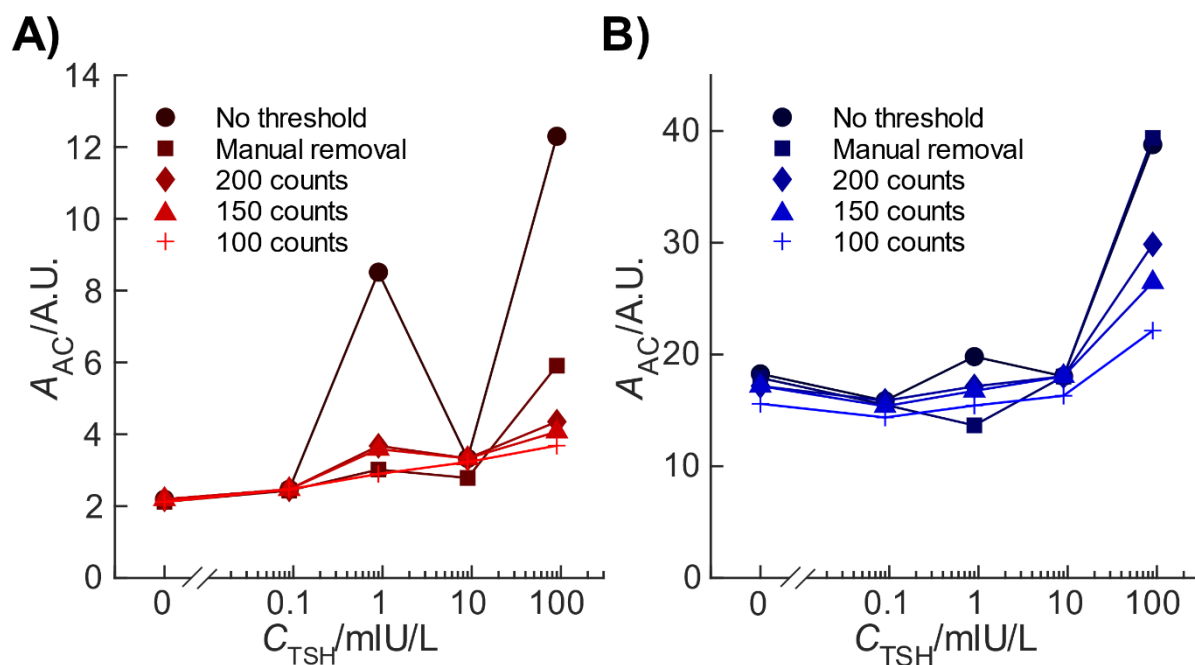


Figure S12. Amplitude of the auto-correlation function of A) erbium and B) thulium at different analyte concentrations and at a low UCNP concentration (3.2 µg/mL) in the TSH immunoassay. There are significant deviations when no threshold is used, while only minor differences are observed when a certain threshold is used.

Table S4. Fitting parameters of the four-parameter logistic functions used to fit the TSH immunoassay standard curves in buffer and plasma with high (72 $\mu\text{g/mL}$) and low (3.2 $\mu\text{g/mL}$) UCNP concentrations. Errors are given as 95% confidence intervals.

	A_1	A_2	c_0 (mIU/L)	p
Buffer (high UCNP)	2.91 (± 1.64)	0.013 (± 0.006)	183.1 (± 158.8)	1.07 (± 0.15)
Plasma (high UCNP)	3.08 (± 22.74)	0.007 (± 0.019)	667.8 (± 7241)	0.91 (± 0.64)
Buffer (low UCNP)	5.24 (± 0.83)	0.007 (± 0.227)	9.84 (± 3.86)	1.23 (± 0.82)
Plasma (low UCNP)	0.82 (± 0.33)	0.083 (± 0.167)	8.22 (± 7.33)	1.82 (± 10.00)

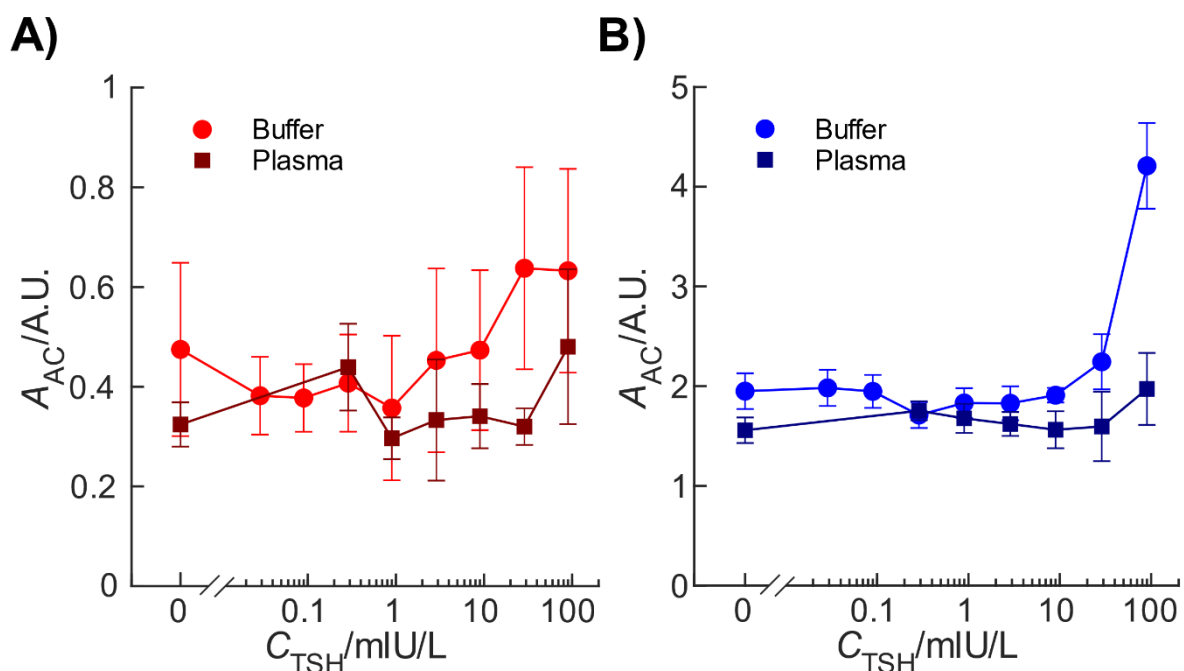


Figure S13. Amplitude from the ACFs of A) Er(3%) and B) Tm(8%) in buffer and plasma at a high UCNP concentration (72 $\mu\text{g/mL}$) in the TSH immunoassay. The A_{AC} values and their error bars represent the averaged amplitudes and standard deviations of six replicate measurements. Measurements were conducted for 150 s.

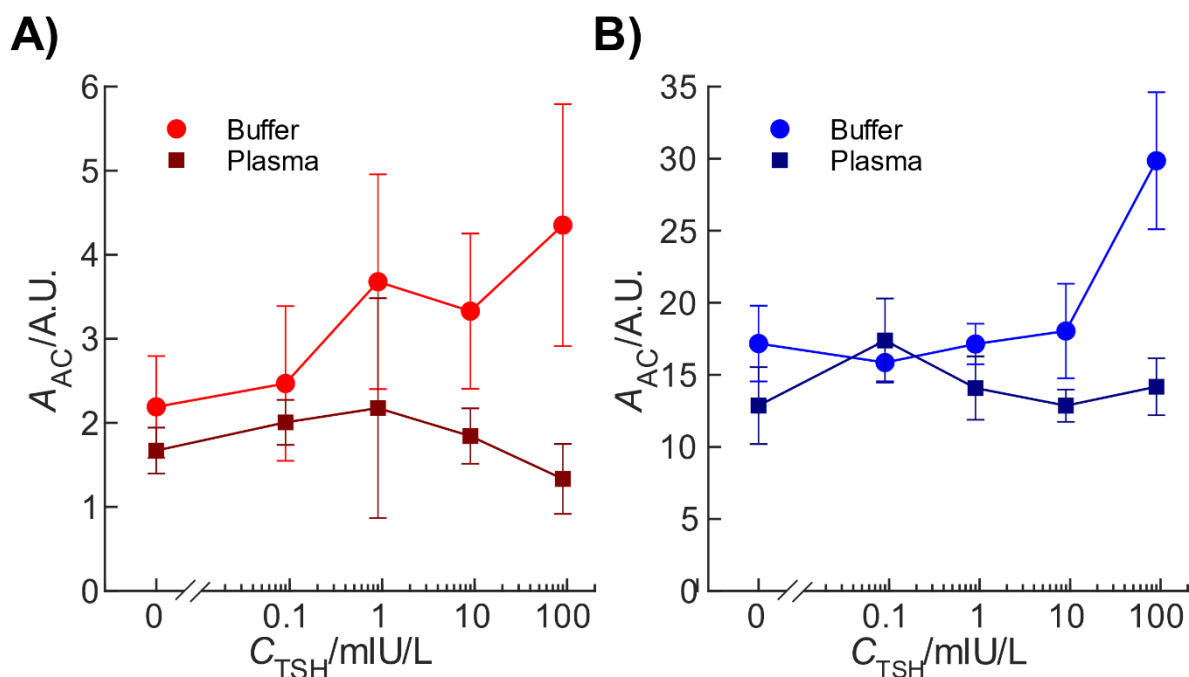


Figure S14. Amplitude from the ACFs of A) Er(3%) and B) Tm(8%) in buffer and plasma at a low UCNP concentration (3.2 $\mu\text{g/mL}$) in the TSH immunoassay. The A_{AC} values and their error bars represent the averaged amplitudes and standard deviations of six replicate measurements. Measurements were conducted for 300 s.

References

1. Lahtinen, S.; Krause, S.; Arppe, R.; Soukka, T.; Vosch, T., Upconversion Cross-Correlation Spectroscopy of a Sandwich Immunoassay. *Chem. – Eur. J.* **2018**, *24* (37), 9229-9233.
2. Hess, S. T.; Huang, S.; Heikal, A. A.; Webb, W. W., Biological and Chemical Applications of Fluorescence Correlation Spectroscopy: A Review. *Biochemistry* **2002**, *41* (3), 697-705.